PHYSICAL REVIEW D **88,** 014038 (2013)

Pion transition form factor in the constituent quark model

A. E. Dorokhov* and E. A. Kuraev†

JINR-BLTP, 141980 Dubna, Moscow Region, Russian Federation

(Received 22 May 2013; published 24 July 2013)

We calculate the transition form factor of the neutral pion where one photon is virtual and another photon is real in the model where the light constituent quark mass and the quark-pion vertex are taken to be momentum independent. Radiative corrections to the lowest order triangle quark Feynman amplitude are calculated. The resummation of the lowest radiative corrections to the virtual photon vertex is done by applying the Sudakov exponential hypothesis. By using fitting parameters, the quark mass and the strong coupling constant, the results on the pion transition form factor are compared with existing data published by CELLO, CLEO, *BABAR*, and Belle collaborations.

DOI: 10.1103/PhysRevD.88.014038 PACS numbers: 13.60.−r, 13.66.Bc, 12.38.Lg, 12.38.Bx

I. INTRODUCTION

Much attention has been paid to the problem of describing the transition form factor of neutral pion. To get new information about the wave function of the neutral pion [1–3], namely, the distribution of the neutral pion light-cone momentum fractions between light u and d quarks, is the motivation for numerous theoretical approaches to describe the transition form factor. Experimental information on the form factor is obtained in the process $e^+e^- \to e^+e^-\pi_0$ (Fig. 1). The kinematics, when one photon is almost real and the other is highly virtual with spacelike momentum transfer squared Q^2,

$$|q_1^2| \approx 0 \ll -q_2^2 = Q^2, \tag{1}$$

was measured by several experimental collaborations: CELLO [4], CLEO [5] at low and intermediate Q^2, and more recently by *BABAR* [6] and Belle [7] at higher Q^2.

The *BABAR* collaboration fitted their experimental results for the form factor multiplied by Q^2 as an increasing function of momentum transfer squared (Fig. 5),

$$Q^2 F^A_{\pi\gamma}(Q^2) = A\left(\frac{Q^2}{10\ \mathrm{GeV}^2}\right)^{\beta}, \tag{2}$$

with

$$A_{BABAR} = 0.182\ \mathrm{GeV}, \qquad \beta_{BABAR} = 0.251, \qquad \chi^2_{BABAR}/[15] = 1.04, \tag{3}$$

$$A_{BABAR+} = 0.182\ \mathrm{GeV}, \qquad \beta_{BABAR+} = 0.252, \qquad \chi^2_{BABAR+}/[35] = 0.87, \tag{4}$$

where in square brackets we point out the number of degrees of freedom. In the first line, only *BABAR* data are taken into account while in the second line the full set from *BABAR*, CLEO and CELLO data are taken into account.

The Belle collaboration considered two parametrizations providing very similar goodness of fit. One is the same as (2) (Fig. 6) and the other corresponds to the constant asymptotic behavior

$$Q^2 F^B_{\pi\gamma}(Q^2) = \frac{B}{1 + \frac{C}{Q^2}}. \tag{5}$$

The corresponding parameters are

$$A_{\mathrm{Belle}} = 0.169\ \mathrm{GeV}, \qquad \beta_{\mathrm{Belle}} = 0.18, \qquad \chi^2_{\mathrm{Belle}}/[13] = 0.429, \tag{6}$$

$$A_{\mathrm{Belle}+} = 0.172\ \mathrm{GeV}, \qquad \beta_{\mathrm{Belle}+} = 0.221, \qquad \chi^2_{\mathrm{Belle}+}/[33] = 0.637, \tag{7}$$

$$B_{\mathrm{Belle}} = 0.209\ \mathrm{GeV}, \qquad C_{\mathrm{Belle}} = 2.2\ \mathrm{GeV}^2, \qquad \chi^2_{\mathrm{Belle}}/[13] = 0.435, \tag{8}$$

$$B_{\mathrm{Belle}+} = 0.186\ \mathrm{GeV}, \qquad C_{\mathrm{Belle}+} = 0.948\ \mathrm{GeV}^2, \qquad \chi^2_{\mathrm{Belle}+}/[33] = 0.733. \tag{9}$$

The data on the pion-photon transition form factor obtained by CELLO, CLEO, *BABAR*, and Belle collaborations attract much attention [8–14] with the aim to extract the pion distribution amplitude, a nonperturbative quantity important in the description of hard exclusive hadronic processes.

The growing behavior of the form factor (2) is in clear contradiction with the prediction of the approach based on the factorization theorem applied to this process (see [8] and references therein). On the other hand, this behavior might indicate a logarithmically enhanced asymptotic behavior of the form factor, as has been argued in [15–19].

In [15], the neutral pion transition form factor was considered in the model with momentum-independent light quark mass and quark-pion vertex. In this model,

*dorokhov@theor.jinr.ru
†kuraev@theor.jinr.ru

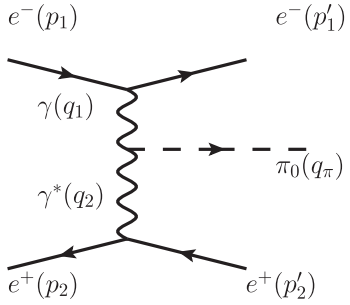

FIG. 1. Neutral pion production in the e^+e^- scattering.

the leading order contribution to the form factor is given by the triangle diagram of Fig. 2. Its asymptotic behavior for the kinematics (1) is a double-logarithmic one [15,18], $\ln^2(Q^2/M_q^2)$, where M_q is the quark mass serving as an infrared cutoff parameter. In order to fit the *BABAR* data, one needs to tune the value of the mass parameter around $M_q \approx 135$ MeV (see below). In [19–21], a more realistic model was considered with the quark mass and quark-pion vertex being momentum dependent. Due to the latter property, the asymptotics of the form factor becomes a single-logarithmic one, $\ln(Q^2/M_q^2)$, in the case of so-called "flat" pion distribution amplitude. In [18], the neutral pion transition form factor has been considered in the leading double-logarithmic approximation in the scattering and annihilation channels.

In the present work, we consider the effect of the lowest-order gluon radiative corrections in the above model. To simplify calculations, only the model with the constant quark mass and quark-pion vertex will be explored. We shall use the well-known expression for the virtual photon-quark vertex (the so-called Sudakov form factor [22]) which enters into the triangle Feynman diagram describing the conversion of two photons to the neutral pseudoscalar meson. The motivation of this and other similar studies is, first, to describe the existing data in the interval of $Q^2 \gtrsim 1$ GeV^2 and, second, to understand if there are any inconsistencies between *BABAR* and Belle data at large $Q^2 \geq 10$ GeV^2.

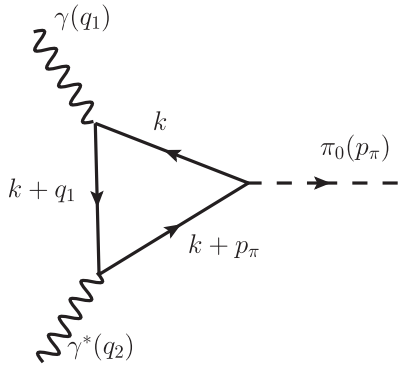

FIG. 2. Lowest-order QCD amplitude—the triangle vertex for $\gamma\gamma^* \to \pi_0$ process.

In Sec. II, both channels of pseudoscalar meson production in electron-proton $e^-p \to e^-p\pi_0$ and electron-positron $e^+e^- \to \pi_0 e^+e^-$ collisions are considered. The second process could be the subject of future experimental investigation. In Secs. III, IV, and V, we discuss the leading order (LO), next-to-leading order (NLO), and the Sudakov exponentiation calculations of the amplitude for the pion-photon transition. In Sec. VI, we compare our model calculations with the existing experimental data.

II. SCATTERING CHANNEL

The matrix element for the neutral pion production in the high-energy electron-proton scattering (replacing the e^+ line in Fig. 1 by the proton p line),

$$e^-(p_1) + p(p_2) \to e^-(p_1') + p(p_2') + \pi_0(p_\pi),$$

can be written as

$$M^{ep\to ep\pi_0} = \frac{F(Q^2)}{q_2^2 q_1^2}\frac{8\alpha^2}{f_\pi} N_e J_\nu(q_2)\epsilon_{\mu\nu\lambda\sigma} p_1^\mu q_2^\lambda q_1^\sigma, \quad (10)$$

for the kinematics of almost forward electron scattering

$$|q_1^2| = |(p_1 - p_1')^2| \ll Q^2 = -q_2^2 = -(p_2 - p_2')^2 \sim s = (p_1 + p_2)^2. \quad (11)$$

In (10), $f_\pi = 92.2$ MeV is the pion decay constant, $N_e = (1/s)\bar{u}(p_1')\hat{p}_2 u(p_1)$, and $F(Q^2)$ is the pion transition form factor.

In the lowest order, the form factor is given by the triangle quark loop integral (Fig. 2)

$$F_0(Q^2) = \int \frac{d^4k}{i\pi^2}\frac{-M_q^2}{(k^2 - M_q^2)((k+q_1)^2 - M_q^2)((k-q_2)^2 - M_q^2)}, \quad (12)$$

$$F_0(0) = -2\frac{M_q^2}{m_\pi^2}\int_0^1 \frac{dx}{x}\ln\left(1 - x(1-x)\frac{m_\pi^2}{M_q^2}\right), \qquad F_0(0) \overset{m_\pi\to 0}{=} 1, \quad (13)$$

where m_π is the pion mass, M_q is the light quark mass parameter, and $J_\nu(q)$ is the current corresponding to the proton vertex

$$J_\nu(q) = \bar{u}(p_2')\Big[2M_P(F_e(q^2) - F_m(q^2))\frac{1}{4M_P^2 - q^2} \times (p_2 + p_2')_\nu + F_m(q^2)\gamma_\nu\Big]u(p_2), \quad (14)$$

where M_P is the proton mass. F_e and F_m are the Sachs electric and magnetic form factors of the proton.

The differential cross section for the process $ep \to ep\pi_0$ has the form

$$d\sigma = \frac{\alpha^4}{\pi^5 f_\pi^2}\frac{|F(Q^2)|^2}{(q_2^2 q_1^2)^2}\Phi(Q^2)\frac{1}{s}\frac{d^3p_1'}{2E_1'}\frac{d^3p_2'}{2E_2'}\frac{d^3p_\pi}{2E_\pi} \times \delta^4(p_1 + p_2 - p_1' - p_2' - p_\pi), \quad (15)$$

with

$$\Phi(Q^2) = \left[\left(\frac{1}{1+\frac{Q^2}{4M_p^2}}(F_e - F_m)^2 + F_m^2\right) \times (p_2 + p_2')_\nu (p_2 + p_2')_{\nu_1} + F_m^2 g_{\nu\nu_1}\right] \times (\nu, p_1, q, q_1)(\nu_1, p_1, q, q_1), \quad (16)$$

where $(\nu, p_1, q, q_1) = \epsilon^{\nu\alpha\beta\gamma} p_{1\alpha} q_\beta q_{1\gamma}$. In the limit of large $Q^2 \sim s$, one has

$$\Phi(Q^2 \sim s) = \frac{1}{4}(sQ^2)^2\left(\frac{1}{1+\frac{Q^2}{4M_p^2}}(F_e(Q^2) - F_m(Q^2))^2 + F_m^2(Q^2)\right). \quad (17)$$

In (15), we use the normalization of the matrix element for the subprocess $\gamma^*\gamma \to \pi^0$ in accordance with the current algebra in the case of two real photons ($q_2^2 = q_1^2 = 0$) [23],

$$M^{\pi_0 \to \gamma_1(q_1\epsilon_1)\gamma_2(q_2\epsilon_2)} = i\frac{\alpha}{\pi f_\pi}(q_1, q_2, \epsilon_1, \epsilon_2), \quad (18)$$

corresponding to the width

$$\Gamma^{\pi_0 \to 2\gamma} = \frac{\alpha^2 m_\pi^3}{64\pi^3 f_\pi^2} \approx 7.1 \text{ KeV}. \quad (19)$$

For the $e^\pm e^- \to \pi_0 e^\pm e^-$ collisions

$$e(p_1^\pm) + e(p_2) \to e(p_1^{\pm\prime}) + e(p_2') + \pi_0(p_\pi),$$

one should put $F_e(Q^2) = F_m(Q^2) = 1$ in the above expressions for Φ.

III. BORN APPROXIMATION

Let us now consider the amplitude $\gamma^*\gamma \to \pi^0$ in the context of the constituent quark model with momentum-independent quark mass M_q [24]. Within this model, the pion form factor is given by the quark-loop (triangle) diagram (Fig. 2). The result for the form factor in the considered asymmetric kinematics ($q_1^2 = 0$, $q_2^2 = -Q^2$) is given by [25]

$$F_0(Q^2) = \frac{1}{Q^2}\frac{m_\pi^2}{1+\frac{m_\pi^2}{Q^2}}\left[\frac{1}{4\arcsin^2(\frac{m_\pi}{2M_q})}\ln^2\frac{\beta_q+1}{\beta_q-1} + 1\right], \quad (20)$$

with $\beta_q = \sqrt{1+\frac{4M_q^2}{Q^2}}$ and the normalization is $F_0(Q^2 = 0) = 1$

In [15], this LO expression was used to explain a growing-type form factor as it was measured by the *BABAR* collaboration [6]. The quark mass was used as the only fitting parameter with the result (see below Table I)

$$M_q \approx 135 \text{ MeV}. \quad (21)$$

The expansion of the log term in the form factor (20) at large $Q^2 \gg M_q^2$ leads to

$$F_0^{\text{as}}(Q^2) = \frac{1}{Q^2}\frac{m_\pi^2}{2\arcsin^2(\frac{m_\pi}{2M_q})} \times \left\{\frac{1}{2}L^2 + 2\arcsin^2\left(\frac{m_\pi}{2M_q}\right) + O\left(\frac{M_q^2}{Q^2}\right)\right\}, \quad (22)$$

where the large logarithm is

$$L = \ln\frac{Q^2}{M_q^2}.$$

Numerically, $F_0^{\text{as}}(Q^2)$ and $F_0(Q^2)$ become indistinguishable at $Q^2 > 1$ GeV^2.

In the following, we would like to understand the role of radiative QCD corrections to the L^2 term in the form factor which are more important at large Q^2 than neglected in (22) power corrections. To this end, we first reproduce the leading L^2 asymptotic term in (22) by using two different techniques which become useful when considering the radiative corrections in the leading logarithmic approximation.

One of these methods consists in joining the denominators of the integrand in (12) by using Feynman parameters and performing the loop momentum integration. In the case of $q_1^2 \to 0$, one obtains

$$F_0(Q^2) = 2\int d^3x\,\delta\left(\sum_{i=1}^3 x_i - 1\right)\frac{M_q^2}{M_q^2 - m_\pi^2 x_1 x_3 + Q^2 x_2 x_3} = \frac{2M_q^2}{Q^2 + m_\pi^2}\int_0^1 \frac{dx}{x}\ln\frac{1+\frac{Q^2}{M_q^2}x(1-x)}{1-\frac{m_\pi^2}{M_q^2}x(1-x)}, = \frac{M_q^2}{Q^2}L^2\left(1 + O\left(\frac{m_\pi^2}{M_q^2}, \frac{M_q^2}{Q^2}\right)\right). \quad (23)$$

TABLE I. One-parameter fit of the *BABAR* and Belle data. In square brackets, the number of degrees of freedom is pointed out.

	BABAR			Belle		
	M_q	χ^2/[16]	$\bar{\chi}^2$	M_q	χ^2/[14]	$\bar{\chi}^2$
LO	0.135	1.697	1.629	0.126	0.696	1.611
NLO	0.149	1.185	1.137	0.142	0.434	1.005
Exp.	0.147	1.196	1.148	0.140	0.478	1.106

An alternative calculation is based on the use of the Sudakov parametrization of the loop momentum

$$k = \alpha\tilde{q}_1 + \beta\tilde{p}_\pi + k_\perp,$$

with $\tilde{q}_1$, $\tilde{p}_\pi$ being the lightlike four vectors constructed from the external momenta, $k_\perp\tilde{q}_1 = k_\perp\tilde{p}_\pi = 0$. By using the known relations

$$\begin{aligned} d^4k &= \frac{Q^2}{2}d\alpha d\beta d^2k_\perp, \\ k_\perp^2 &= -\vec{k}^2, \\ k^2 - M_q^2 + i0 &= Q^2\alpha\beta - \vec{k}^2 - M_q^2 + i0, \\ (k+q_1)^2 - M_q^2 &= -Q^2\beta(1-\alpha) - \vec{k}^2 - M_q^2, \\ (k-q)^2 - M_q^2 &= -Q^2\alpha(1-\beta) - \vec{k}^2 - M_q^2, \end{aligned} \tag{24}$$

and performing the integration in $\vec{k}^2$ by the relation

$$\int \frac{d\vec{k}^2}{Q^2\alpha\beta - \vec{k}^2 - M_q^2 + i0} = -i\pi\Theta(Q^2\alpha\beta - M_q^2),$$

we obtain

$$F_0^{\rm as}(Q^2) = \frac{2M_q^2}{Q^2}\int_{M_q^2/Q^2}^1 \frac{d\alpha}{\alpha}\int_{M_q^2/(Q^2\alpha)}^1 \frac{d\beta}{\beta} = \frac{M_q^2}{Q^2}L^2.$$

Here, we also take into account both possibilities of positive and negative values of the Sudakov parameters α, β. Below, we shall use both the Feynman and Sudakov approaches.

IV. LOWEST-ORDER QCD RADIATIVE CORRECTIONS

The lowest-order QCD corrections include three vertex subgraphs and three quark self-energy subgraphs (Fig. 3). The kinematics of the main contributions of the Feynman triangle amplitude correspond to the "almost on-mass-shell" quark connecting the almost on-mass-shell photon and the emission of a real pion, while the two other quark lines are essentially off mass shell. Thus, one of the vertex functions associated with the off-mass-shell external photon underlies the Sudakov conditions: both quarks are off mass shell. The two other vertices describe the situation when the photon and one of the quarks are almost on mass shell, while the other quark is off mass shell. This configuration corresponds to the so-called Landau case [26]. The contribution from the triangle amplitude with a mass operator insertion to the "almost real" quark line does not contain logarithmically enhanced terms.

Consider first the vertex subgraph with an external highly virtual photon with momentum q_2. The corresponding vertex function has the form [see Fig. 4(a)]

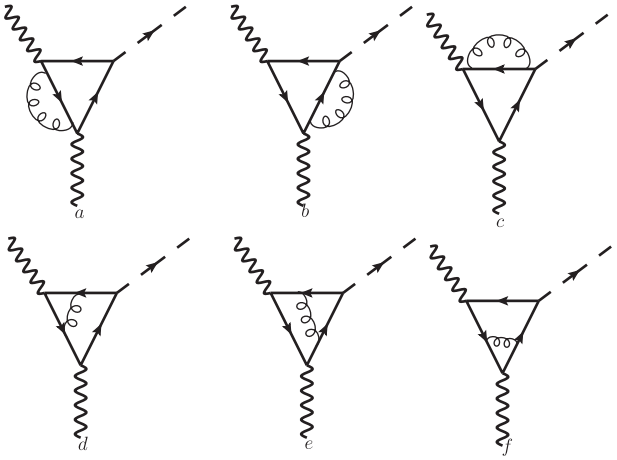

FIG. 3. Next-to-leading QCD radiative corrections to the triangle amplitude for the $\gamma\gamma^* \to \pi_0$ process.

$$V_\mu(Q^2) = \frac{\alpha_s C_F}{4\pi}\int\frac{d^4\kappa}{i\pi^2} \times \frac{N_\mu}{\kappa^2((p_1-\kappa)^2 - M_q^2)((p_2-\kappa)^2 - M_q^2)}, \tag{25}$$

$$\begin{aligned} N_\mu &= \bar{u}(p_2)\gamma_\lambda(\hat{p}_2 - \hat{\kappa} + M_q)\gamma_\mu(\hat{p}_1 - \hat{\kappa} + M_q)\gamma^\lambda u(p_1), \\ Q^2 &= 2p_1p_2 \gg |p_1^2|, |p_2^2| \gg M_q^2. \end{aligned} \tag{26}$$

Here, $C_F = 4/3$ is the Casimir invariant of the SU(3) color group.

The logarithmically enhanced contributions arise from two kinematically different regions of virtual gluon momentum squared $|\kappa^2|$, corresponding to small and large values of $|\kappa^2|$. Using the Sudakov parametrization

$$\kappa = \alpha_1 p_2' + \beta_1 p_1' + \vec{\kappa}_\perp, \qquad \kappa^2 = Q^2\alpha_1\beta_1 - \vec{\kappa}^2,$$
$$d^4\kappa = \pi\frac{Q^2}{2}d\alpha_1 d\beta_1 d\vec{\kappa}^2,$$

with p_1', p_2' lightlike 4 vectors built from p_1, p_2, we write N_μ, in the limit (26), as

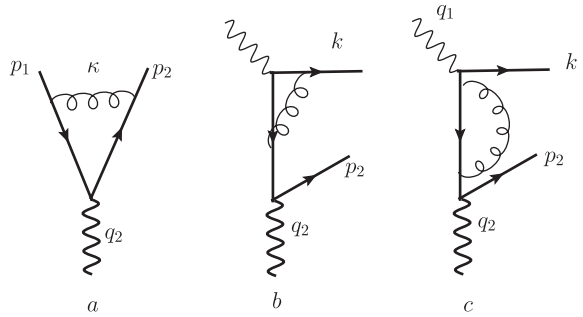

FIG. 4. Lowest-order QCD radiative correction to the subgraphs with vertices and mass operators.

$$N_\mu = [2Q^2(1-\alpha_1)(1-\beta_1)+\kappa^2]J_\mu,$$

with

$$J_\mu = \bar{u}(p_2)\gamma_\mu u(p_1).$$

For the first term in the square brackets of N_μ, we obtain (small $|\kappa^2|$ region)

$$V_{1\mu}(Q^2;\alpha,\beta) = -2\frac{\alpha_s C_F}{4\pi}J_\mu\int_0^1\frac{d\alpha_1(1-\alpha_1)}{\alpha_1+\alpha}\times\int_0^1\frac{d\beta_1(1-\beta_1)}{\beta_1+\beta}\theta(Q^2\alpha_1\beta_1-M_q^2) = -\frac{\alpha_s C_F}{2\pi}[\ln\alpha\ln\beta+\ln(\alpha\beta)]J_\mu, \quad (27)$$

where factor 2 is due to the two regions of negative and positive values of the Sudakov parameters. In the derivation of (27), we used the relations $|p_1^2/Q^2| = |\alpha|$, $|p_2^2/Q^2| = |\beta|$, with α, β being the Sudakov variables associated with the loop momentum of the quark loop.

The contribution from the region with large $|\kappa^2|$ comes from the second term in the square brackets of N_μ,

$$V_{2\mu}(Q^2) = -\frac{\alpha_s C_F}{4\pi}J_\mu\int\frac{d^4\kappa}{i\pi^2}\times\frac{1}{((p_1-\kappa)^2-M_q^2)((p_2-\kappa)^2-M_q^2)}.$$

Here we have to introduce the ultraviolet cutoff parameter Δ, such as $|\kappa^2|<\Lambda^2$. The usual procedure of joining the denominators and performing the integration leads to

$$V_{2\mu}(Q^2) = -\frac{\alpha_s C_F}{4\pi}J_\mu\int_0^1 dx\int\frac{d^4\kappa}{i\pi^2}\times\frac{1}{[(\kappa-p_x)^2-Q^2x(1-x)]^2} = -\frac{\alpha_s C_F}{4\pi}J_\mu\ln\frac{\Lambda^2}{Q^2}, \quad (28)$$

where $p_x = xp_1+(1-x)p_2$. Note that we systematically omit the logarithmically suppressed terms. After regularization, the cutoff parameter must be replaced by the quark mass.

The total answer for V_μ is

$$V_\mu(Q^2;\alpha,\beta) = -\frac{\alpha_s}{2\pi}C_F\left[\ln\alpha\ln\beta+\ln(\alpha\beta)+\frac{1}{2}L\right]J_\mu. \quad (29)$$

The contribution of other Feynman amplitudes [Figs. 4(b) and 4(c)] does not contain logarithmic enhancement. We will illustrate this statement in the framework of QED [26,27]. Let us consider the contribution of two remaining diagrams with one vertex function [Fig. 4(b)] and mass operator insertion [Fig. 4(c)],

$$V_{\mu,\nu} = -4\pi\alpha_s C_F\bar{u}(p_2)\gamma_\mu\left[\frac{1}{t}(\hat{p}_2-\hat{q}_2+M_q)\hat{\Gamma}_\nu + \frac{\hat{M}(p_2-q_2)}{(\hat{p}_2-\hat{q}_2-M_q)^2}\gamma_\nu\right]u(k),$$
$$t = (p_2-q_2)^2-M_q^2, \qquad p_2-q_2 = q_1-k. \quad (30)$$

Using the explicit expressions for the vertex Γ_ν and mass operator $\hat{M}(p)$ given in the Appendix, we obtain

$$V_{\mu\nu} = -\frac{2\alpha^2 i}{M_q}\bar{u}(p_2)\gamma_\mu\times\left[A_1\left(\gamma_\nu-\hat{q}_1\frac{1}{kq_1}k_\nu\right)+A_2\frac{1}{M_q}\hat{q}_1\gamma_\nu\right],$$

where

$$A_1 = \frac{1}{2(\tilde{t}+1)}\left[1-\frac{\tilde{t}}{\tilde{t}+1}l_t\right], \qquad \tilde{t} = \frac{t}{M_q^2}, \qquad l_t = \ln\frac{-t}{M_q^2}.$$

We see that the relevant contribution is suppressed by a small factor $1/\tilde{t}$. Other terms do not contribute to the amplitude. A similar statement is valid for two remaining diagrams [see Figs. 3(b) and 3(e)].

Collecting all logarithmically enhanced contributions, we finally obtain

$$\int_{M_q^2/Q^2}^1\frac{d\alpha}{\alpha}\int_{M_q^2/(Q^2\alpha)}^1\frac{d\beta}{\beta}\left(1-\frac{\alpha_s}{2\pi}\times C_F\left[\ln\alpha\ln\beta+\ln(\alpha\beta)+\frac{1}{2}\ln\frac{Q^2}{M_q^2}\right]\right) = \frac{1}{2}L^2-\frac{\alpha_s C_F}{2\pi}\frac{1}{12}L^3\left(\frac{1}{2}L-1\right). \quad (31)$$

Thus, the form factor at large Q^2 (22), modified by the NLO radiative QCD corrections, becomes

$$F_1^{\rm as}(Q^2) = \frac{1}{Q^2}\frac{m_\pi^2}{2\arcsin^2\left(\frac{m_\pi}{2M_q}\right)}\left\{\frac{1}{2}L^2-\frac{\alpha_s}{24\pi}C_F L^3\left(\frac{1}{2}L-1\right)+2\arcsin^2\left(\frac{m_\pi}{2M_q}\right)\right\}. \quad (32)$$

V. HIGHER-ORDER QCD GENERALIZATION

In order to estimate the effect of the higher orders of the QCD perturbation theory, we apply to the next-to-leading logarithmic approximation (31), the Sudakov exponentiation hypothesis, with the result

$$\int_{M_q^2/Q^2}^1 \frac{d\alpha}{\alpha} \int_{M_q^2/(Q^2\alpha)}^1 \frac{d\beta}{\beta} \exp\left\{-\frac{\alpha_s}{2\pi} C_F \left[\ln\alpha \ln\beta + \ln(\alpha\beta) + \frac{1}{2}L\right]\right\} \tag{33}$$

$$= \frac{1}{\rho} e^{-\frac{1}{2}L\rho} \int_0^1 \frac{dx}{x-\frac{1}{L}} e^{xL\rho}(1 - e^{-L^2\rho(1-x)(x-\frac{1}{L})}), \tag{34}$$

where $\rho = \frac{\alpha_s}{2\pi} C_F$. For the form factor, the resummation effects lead to the generalization of (32) as

$$F_{\exp}^{\text{as}}(Q^2) = \frac{1}{Q^2} \frac{m_\pi^2}{2\arcsin^2(\frac{m_\pi}{2M_q})} \cdot \left\{\frac{1}{\rho} e^{-\frac{1}{2}L\rho} \int_0^1 \frac{dx}{x-\frac{1}{L}} \times e^{xL\rho}(1 - e^{-L^2\rho(1-x)(x-\frac{1}{L})}) + 2\arcsin^2\left(\frac{m_\pi}{2M_q}\right)\right\}. \tag{35}$$

It is important to note that the exponent factor under integral in (33) is in full agreement with the results obtained in QED [22,28] and QCD [29,30] for the summation of the leading and next-to-leading double logarithmic corrections to the Sudakov form factor. This fact confirms the correctness of our calculations.

VI. THE RESULTS AND DISCUSSION

There are two parameters within the parametrization of the pion transition form factor suggested by the quark model with radiative corrections. They are the quark mass M_q and the strong coupling constant α_s. We try to fit the experimental data for the form factor by varying these parameters. The results of the fit are presented in Tables I, II, and III and Figs. 5 and 6.

In the fitting procedure, we use the parametrizations (2) and (5) as reference parametrizations. From the corresponding goodness of fit (3), (4), (6), and (7), one concludes, first, that $\chi^2_{BABAR} > \chi^2_{\text{Belle}}$ and, second, that the data set extended by experimental points of CELLO and CLEO is $\chi^2_{BABAR} > \chi^2_{BABAR+}$ and $\chi^2_{\text{Belle}} < \chi^2_{\text{Belle}+}$. The first fact is due to systematically lower error bars for the *BABAR* point set than for the Belle. The second property is interpreted as an indication of better consistency of the *BABAR* data with the previous data at lower Q^2 than for the Belle data.[1]

First of all, let us use our model to fit the *BABAR* and Belle data considering the quark mass as a free parameter and the strong coupling to be fixed at $\alpha_s = 0.35$, which corresponds to a renormalization scale of about 1 GeV. The results are given in Table I. For the LO fit, we use expression (22), for the NLO fit we use expression (32), and the Sudakov resummed expression (Exp.) is (35). In order to compare goodness of fit based on data used from different collaborations we introduce the relative parameter

[1]At this point, we disagree with the conclusions made in [31].

TABLE II. One-parameter fit of the *BABAR* and Belle data including also the data from the CELLO and CLEO collaborations. In square brackets, the number of degrees of freedom is pointed out.

	BABAR+			Belle+		
	M_q	χ^2/[36]	$\bar{\chi}^2$	M_q	χ^2/[34]	$\bar{\chi}^2$
LO	0.136	2.377	2.732	0.133	2.891	4.538
NLO	0.150	1.487	1.709	0.147	1.684	2.644
Exp.	0.148	1.587	1.824	0.145	1.878	2.948

TABLE III. Two-parameter fit of the *BABAR* and Belle data. In square brackets, the number of degrees of freedom is pointed out.

	BABAR				Belle			
	M_q	α_s	χ^2/[15]	$\bar{\chi}^2$	M_q	α_s	χ^2/[13]	$\bar{\chi}^2$
NLO	0.149	0.349	1.264	1.215	0.149	0.505	0.428	0.998
Exp.	0.152	0.513	1.187	1.196	0.159	0.963	0.422	0.984

$$\bar{\chi}^2 = \chi^2/\chi_a^2, \tag{36}$$

where a is for *BABAR* or Belle based data set. In (36), χ^2 is for our model and for the powerlike fits χ_a^2 is from (3), (4), (6), and (7), respectively.

From Table I, one finds that the goodness of fit becomes better when going from the LO fit to the NLO fit and almost does not change after the Sudakov resummation.

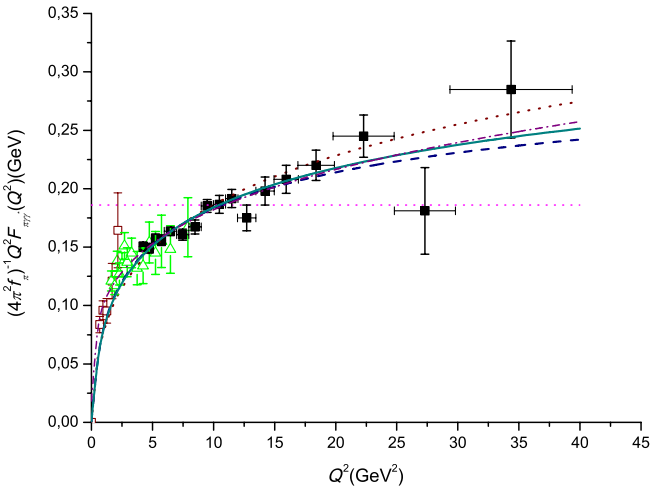

FIG. 5 (color online). The fit of our model for the cases of the LO approximation [Eqs. (22), dotted line]; the NLO approximation [Eq. (32), dashed line); the resummation approximation [Eq. (35), solid line) for the π^0 form factor and its comparison with the experimental data of the CELLO [4] (open boxes), CLEO [5] (open triangles), and *BABAR* [6] (filed boxes) collaborations. The dashed-dotted line shows the fit of the data by the *BABAR* collaboration.

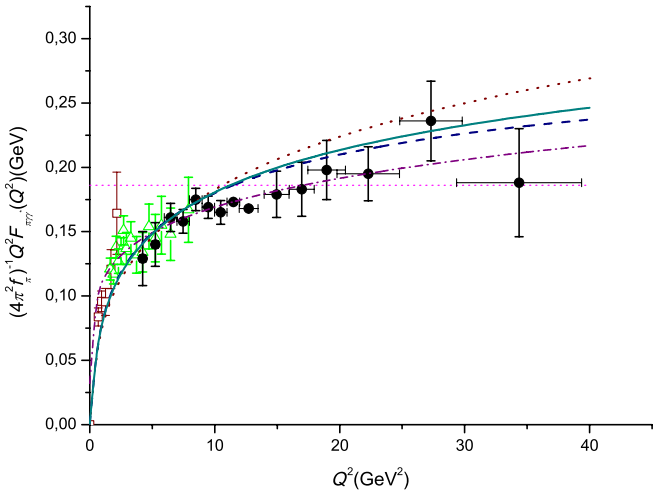

FIG. 6 (color online). The fit of our model in the cases of the LO approximation [Eqs. (22), dotted line); the NLO approximation [Eq. (32), dashed line]; the resummation approximation [Eq. (35), solid line)] for the π^0 form factor and its comparison with the experimental data of the CELLO [4] (open boxes), CLEO [5] (open triangles), and Belle [7] (filled circles) collaborations. The dashed-dotted line shows the fit of the data by the Belle collaboration.

This justifies our model with radiative corrections. At the same time, the parameter M_q becomes higher.

In Table II, we made a fit of the *BABAR* and Belle data including also the set of points from the CELLO and CLEO collaborations. We see that, qualitatively, for our model, the situation does not change too much and the value of M_q is practically the same for both the cases. The latter fact is rather important. It means that the fit procedure is basically related to the data points at intermediate Q^2 in the region from 5 to 10 GeV^2 where the data are more precise and consistent for all collaborations. At the same time, the region of higher Q^2 (15–40 GeV^2) is less important for the fit. The form factor $F_{\pi\gamma\gamma^*}(Q^2)$ in accordance with different parameterizations given in Table II is drawn in Figs. 5 and 6. In these figures, we also present powerlike fits to the *BABAR* and Belle data (3) and (6), respectively.

In Table III, we made a two-parametric fit to the *BABAR* and Belle data. We see that such a two-parametric fit has equal or even lower χ^2 with respect to the corresponding numbers in Table I. However, the price for that is the growth of the parameter α_s, especially in the case of Belle data. We consider such parametrization as not very physical.

VII. CONCLUSIONS

In the present work, we calculated the transition form factor of the neutral pion where one photon is virtual and the other photon is real in the framework of the model where the light constituent quark mass and the quark-pion coupling are momentum independent.[2] We generalized the previous leading order results [15,18] obtained by considering the triangle diagram by including the radiative gluonic corrections to the first order in perturbation theory.[3] The effect of higher-order radiative corrections to the virtual photon vertex is estimated by applying the Sudakov exponentiation hypothesis. The results obtained are compared with the existing experimental data on the pion transition form factor published by the CELLO, CLEO, *BABAR*, and Belle collaborations.

In general, the model considered contains two parameters: the quark mass M_q and the strong coupling constant α_s.

First, we fit the data at fixed α_s varying only M_q. Taking into account the radiative corrections increases the fitting parameter a little up to $M_q \approx 150$ MeV and improves the goodness of fit. Considering separately the fit of *BABAR* and Belle data (Table I), one gets very close $\bar{\chi}^2$ and the difference in M_q is less than 10 MeV. Including also lower momentum data from CELLO and CLEO (Table II) leads to the inequality $\bar{\chi}^2_{BABAR+} < \bar{\chi}^2_{\text{Belle}+}$ and almost coinciding M_q. In our opinion, it means that the fitting procedure is most sensitive to the intermediate momentum interval, where both the sets of data are in agreement. As for parametrizations discussed in Introduction, *BABAR* data turn out to be more in accordance with lower momentum data than the Belle data. Our model is closer to the tendency of the *BABAR* data. The resummation effects do not lead to significant changes in the goodness of fit comparing with the NLO results.

Second, we try to fit data varying both the model parameters (Table III). The fit of data becomes better, especially in the region of large Q^2. However, α_s has a tendency to be close to unity. This fact is considered as not physically justified and thus not taken into account in our final results.

Let us emphasize that at the moment there are two sets of experimental data (*BABAR* and Belle) on the pion-photon transition form factor at high Q^2. They are fully consistent in the range of momentum transfer squared $Q^2 \sim [5-10]$ GeV^2, but have a different tendency at higher Q^2. Conditionally, the *BABAR* data show "growing" behavior at large Q^2 [see (2)], while the Belle data can be interpreted in a two-fold way as "quasigrowing-quasiconstant" [see (2) and (5)]. From an experimental point of view, the data in the range $Q^2 \sim [15-40]$ GeV^2 are consistent at the level of 1σ standard deviation.

[2]A similar model was considered in [32–34] in view of calculations of hadronic corrections to the muon anomalous magnetic moment.

[3]The problem of radiative corrections to the pion transition form factor was considered some time ago in [35–37] within the factorization approach with massless quarks. In this case, the "large logarithms" $\log Q^2/\mu^2$ contain the QCD scale parameter μ.

However, from a theoretical point of view there are big debates on this difference [8–19]. It is clear that only new high-statistic experiments can resolve this problem.

The emergence of growing data was so unexpected that, at first glance, it seemed that it was impossible to explain such behavior from the field theoretical point of view. However, in [15–19] there was noted that if such growing behavior exists, then it may be related to unusual properties of the pion distribution amplitude in the vicinity of its edge points. This behavior was conditionally called "flat." In this case, the inverse moment of the pion distribution amplitude is not well defined. In particular, such behavior may be modeled if to assume that the pion is almost structureless. In [15] (and later in some other works), it was shown that *BABAR* data can be described in the model with momentum-independent quark mass and quark-pion coupling by using only one parameter: the constituent quark mass M_q if its value is taken as $M_q \approx 135$ MeV. This number was considered as rather small from a phenomenological point of view. One of the main motivations of the present work is to see how sensitive this parameter is to gluonic radiative corrections when fitting the *BABAR* and Belle data. The result is that the mass parameter becomes a bit heavier $M_q \approx 150$ MeV and the quality of fit becomes better.

As it was shown in [19,20], a more advanced model, with momentum-dependent quark mass and quark-pion vertex, has the same qualitative features as the model considered in this work. In the model [19,20], the softened quark propagator and quark-pion vertex lead to the single logarithmic asymptotic dependence on Q^2 instead of the double logarithmic behavior, if the quark-pion vertex is such that it corresponds to the flat pion distribution amplitude. The pion distribution amplitude can even vanish at the end points but still simulates the logarithmic growth in rather a wide range of momentum transfer including its quite large values. When fitting *BABAR* data, the mass parameter is still close to 135 MeV. The calculations given in the present paper can be extended by consideration of not only a momentum-dependent nonperturbative quark propagator and quark-pion vertex but also a momentum-dependent nonperturbative gluon propagator.

Finally, note that there are available data obtained by the *BABAR* collaboration for the η, η' and η_c transition form factors. The comparison of our model calculations with data for these mesons is given in [21]. From our point of view the data show a tendency that with increase of the meson mass the form factor changes its behavior from the growing regime to the "constant" regime. In the framework of our model, this change of behavior is related to a strong dependence of the shape of the meson distribution amplitude on the meson mass. With growing meson mass the meson distribution amplitude changes its shape from the flat shape to the "δ-function" one for heavy mesons [21].

The study of the present work shows that the inclusion of the QCD corrections is essential in the interpretation of experimental data on the pion transition form factor.

ACKNOWLEDGMENTS

We thank Yu. M. Bystritsky, V. V. Bytev, N. I. Kochelev, and Yu. S. Surovtcev for their interest in the subject of the present work and discussions. This work is supported in part by the Russian Foundation for Basic Research (Project No. 11-02-00112).

APPENDIX

The explicit expressions for the vertex function in the Landau kinematics and the mass operator are [26,27]

$$\hat{\Gamma}_\nu = \frac{\alpha}{M_q \pi}\left[a k_\nu + b M_q \gamma_\nu + c \frac{k_\nu}{M_q}\hat{q}_1 + d \hat{q}_1 \gamma_\nu \right], \tag{A1}$$

$$\hat{M}(p) = \frac{\alpha}{2M_q \pi}\left[-a + f \frac{1}{M_q}(\hat{p} + M_q) \right](\hat{p} - M_q)^2, \tag{A2}$$

with $\tilde{t} = t/M_q^2$, $t = (p_2 - q)^2 - M_q^2 = (p_1 - q_1)^2 - M_q^2$, $l_t = \ln(-\tilde{t})$ and the coefficients are

$$\begin{aligned}
a &= -\frac{1}{2(\tilde{t}+1)}\left(1 - \frac{3\tilde{t}+2}{\tilde{t}+1} l_t\right), \\
b &= -1 - \ln\frac{\lambda}{M_q} - \frac{1}{2\tilde{t}} R + \frac{\tilde{t}+2}{4(\tilde{t}+1) l_t}, \\
c &= -\frac{1}{\tilde{t}^2} R - \frac{\tilde{t}+2}{2\tilde{t}(\tilde{t}+1)} + \frac{(\tilde{t}+2)(2\tilde{t}+1)}{2\tilde{t}(\tilde{t}+1)^2} l_t, \\
d &= -\frac{1}{2(\tilde{t}+1)} l_t, \\
f &= \frac{1}{\tilde{t}}\left(1 + 2\ln\frac{\lambda}{M_q} + \frac{\tilde{t}+2}{2(\tilde{t}+1)} + \frac{\tilde{t}^2 - 4\tilde{t} - 4}{2(\tilde{t}+1)^2} l_t\right), \\
R &= \frac{\pi^2}{6} - \mathrm{Li}_2(\tilde{t}+1).
\end{aligned} \tag{A3}$$

Note that the fictive photon mass λ, introduced here, disappears from the final answer.

[1] V. L. Chernyak and A. R. Zhitnitsky, JETP Lett. **25**, 510 (1977).
[2] G. P. Lepage and S. J. Brodsky, Phys. Lett. **87B**, 359 (1979).
[3] A. V. Efremov and A. V. Radyushkin, Phys. Lett. **94B**, 245 (1980).
[4] H. J. Behrend *et al.* (CELLO Collaboration), Z. Phys. C **49**, 401 (1991).
[5] J. Gronberg *et al.* (CLEO Collaboration), Phys. Rev. D **57**, 33 (1998).
[6] B. Aubert *et al.* (*BABAR* Collaboration), Phys. Rev. D **80**, 052002 (2009).
[7] S. Uehara *et al.* (Belle Collaboration), Phys. Rev. D **86**, 092007 (2012).
[8] S. V. Mikhailov and N. G. Stefanis, Nucl. Phys. **B821**, 291 (2009).
[9] S. J. Brodsky, F.-G. Cao, and G. F. de Teramond, Phys. Rev. D **84**, 033001 (2011).
[10] E. R. Arriola and W. Broniowski, Phys. Rev. **81**, 094021 (2010).
[11] S. Noguera and V. Vento, Eur. Phys. J. A **46**, 197 (2010).
[12] S. S. Agaev, V. M. Braun, N. Offen, and F. A. Porkert, Phys. Rev. D **83**, 054020 (2011).
[13] P. Kroll, Eur. Phys. J. C **71**, 1623 (2011).
[14] Y. Klopot, A. Oganesian, and O. Teryaev, Phys. Rev. D **87**, 036013 (2013).
[15] A. E. Dorokhov, Phys. Part. Nucl. Lett. **7**, 229 (2010).
[16] A. V. Radyushkin, Phys. Rev. D **80**, 094009 (2009).
[17] M. V. Polyakov, JETP Lett. **90**, 228 (2009).
[18] Yu. M. Bystritskiy, V. V. Bytev, E. A. Kuraev, and A. N. Ilyichev, Phys. Part. Nucl. Lett. **8**, 73 (2011).
[19] A. E. Dorokhov, JETP Lett. **92**, 707 (2010).
[20] A. E. Dorokhov, arXiv:1003.4693.
[21] A. E. Dorokhov, Nucl. Phys. B, Proc. Suppl. **225**, 141 (2012).
[22] V. V. Sudakov, Zh. Eksp. Teor. Fiz. **30**, 87 (1956) [Sov. Phys. JETP **3**, 65 (1956)].
[23] L. B. Okun, *Leptons and Quarks* (Nauka, Moscow, 1981).
[24] S. B. Gerasimov, Yad. Fiz. **29**, 513 (1979) [Sov. J. Nucl. Phys. **29**, 259 (1979)]; JINR-E2-11693, 1979.
[25] L. Ametller, L. Bergstrom, A. Bramon, and E. Masso, Nucl. Phys. **B228**, 301 (1983).
[26] A. I. Akhiezr and V. B. Berestetskij, *Quantum Electrodynamics*, (Nauka, Moscow, 1981).
[27] E. A. Kuraev, N. P. Merenkov, and V. S. Fadin, Yad. Fiz. **42**, 782 (1987) [Sov. J. Nucl. Phys. **45**, 486 (1987)].
[28] S. Ya. Guzenko, Zh. Eksp. Teor. Fiz. **44**, 1687 (1963).
[29] J. M. Cornwall and G. Tiktopoulos, Phys. Rev. D **13**, 3370 (1976).
[30] J. Frenkel and J. C. Taylor, Nucl. Phys. **B116**, 185 (1976).
[31] N. G. Stefanis, A. P. Bakulev, S. V. Mikhailov, and A. V. Pimikov, Phys. Rev. D **87**, 094025 (2013).
[32] D. Greynat and E. de Rafael, J. High Energy Phys. 07 (2012) 020.
[33] A. A. Pivovarov, Yad. Fiz. **66**, 934 (2003) [Phys. At. Nucl. **66**, 902 (2003)].
[34] R. Boughezal and K. Melnikov, Phys. Lett. B **704**, 193 (2011).
[35] E. Braaten, Phys. Rev. D **28**, 524 (1983).
[36] F. del Aguila and M. K. Chase, Nucl. Phys. **B193**, 517 (1981).
[37] E. P. Kadantseva, S. V. Mikhailov, and A. V. Radyushkin, Yad. Fiz. **44**, 507 (1986) [Sov. J. Nucl. Phys. **44**, 326 (1986)].